



Lasers in Manufacturing Conference 2017

# High-power laser surface processing for fast, reliable repair preparation of CFRP

Hagen Dittmar<sup>a,\*</sup>, Sven Bluemel<sup>a</sup>, Peter Jaeschke<sup>a</sup>, Oliver Suttmann<sup>a</sup>, Ludger Overmeyer<sup>a,b</sup>

<sup>a</sup>Laser Zentrum Hannover e.V., Hollerithallee 8, 30419 Hannover, Germany

<sup>b</sup>Leibniz Universität Hannover, Institut für Transport- und Automatisierungstechnik, An der Universität 2, 30823 Garbsen, Germany

---

## Abstract

As various industries, especially aviation and automotive, are applying an increasing amount of parts fabricated from carbon fibre reinforced plastics (CFRP), proper maintenance and repair procedures are gaining importance, too.

The laser is a potential tool to assist the CFRP repair process by scarfing the damage zone during the repair preparation phase.

This study presents a high-power (1.5 kW) nanosecond pulsed laser for this task. Its performance is evaluated in terms of processing time, bulk material removal rate and formation of a heat affected zone.

The results of the evaluation show that these lasers pose a serious challenge to conventional tools, especially in combination with additional supportive techniques for process automation.

Keywords: laser scarfing; CFRP; repair preparation; automation

---

## 1. Motivation / State of the Art

Laser processing of fibre reinforced composites and especially CFRP has been a target of research activities during the last decades. Their supreme characteristics in regard to lightweight applications have drawn a lot of attention not only to representatives of the aviation industry but recently also to the

---

\* Corresponding author. Tel.: +49 (0) 511 2788-335; fax: +49 (0) 511 2788-100.  
E-mail address: h.dittmar@lzh.de.

automobile industry. However, processing of CFRP utilising conventional tools meets several challenges, which are sought to be solved by laser technology.

Challenges like the heterogeneous setup of CFRP parts and the hardness of carbon fibres cause reduced process precision and increased tool wear. Especially during composite repair or rework, when big amounts of matrix and fibre material need to be removed, tool wear becomes excessive. Laser technology with its contact-free functional principle does not suffer the material related tool wear and offers high precision during CFRP processing as was shown by Dittmar, Gäbler, and Stute, 2013. However, laser material processing is a thermal treatment and deposition of excess heat in CFRP causes heat affected zones (HAZ) that potentially weaken the composite part. Wolynski et al., 2011 demonstrated that the heat affected zone can be significantly reduced by use of short or ultra-short pulsed lasers.

These pulsed lasers only provided small amounts of average power, thus process efficiency was low in comparison to conventional tooling. But with recent developments in laser technology this is about to change: Stolzenburg et al., 2014 showed in a study the possibility to design nanosecond pulsed lasers with good beam quality and high average power up to  $P_{L,avg} = 4.2$  kW in NIR-range. TRUMPF designed a nanosecond pulsed thin disk laser with an average power of  $P_{L,avg} = 1.5$  kW and a maximum available pulse energy of  $E_p = 80$  mJ.

While the increased process efficiency and quality of this laser was already demonstrated for laser cutting/trimming of CFRP by Bluemel et al., 2016, it is still due for laser based bulk material removal.

Bulk material removal is needed during composite repair or rework preparation. Damaged CFRP parts are scarfed either in a stepped or ramped pattern with the scarf area extending largely beyond the size of the actual damage. Therefore, a huge volume of CFRP needs to be removed by laser. Earlier works like Kremser et al., 2014 and Zahedi et al., 2015 investigated laser based composite repair preparation with nanosecond pulsed lasers. Those results mentioned removal rates of  $V_s > 1.67$  mm<sup>3</sup>/s and  $V_s = 1.8$  mm<sup>3</sup>/s respectively. Neither reported any detectable HAZ.

This article studies the new high-power laser's performance during scarfing of CFRP. The focus lies on the material removal, processing time, and detection of a HAZ.

## Nomenclature

#	-	number of repetitions
$A_{cross}$	mm <sup>2</sup>	sample size for micro-cross-sections
$A_{init}$	mm <sup>2</sup>	initial sample size
$A_{proc}$	mm <sup>2</sup>	area of ablation
$A_{sf}$	mm <sup>2</sup>	scan field area
d	mm	sheet thickness
$d_f$	μm	optical fibre diameter
$d_{focal}$	mm	focal diameter
$E_p$	mJ	pulse energy
f	kHz	pulse repetition frequency
h	μm	hatch distance
$l_f$	mm	focal length
λ	nm	wavelength
m	g	initial mass
$P_{L,avg}$	kW	maximum average laser output power
ρ	mg/mm <sup>3</sup>	density
t	s	process time

$t_b$	s	break time
$t_p$	ns	pulse duration
$V$	$\text{cm}^3$	volume
$V_r$	$\text{mm}^3$	removed volume
$V_s$	$\text{mm}^3/\text{s}$	material removal rate
$v$	m/s	scanning velocity

## 2. Experimental

The experiments were conducted with a nanosecond pulsed fibre guided thin-disk laser source by TRUMPF Laser GmbH. The laser source provides a maximum available pulse energy of  $E_p = 80$  mJ and a maximum average laser power of  $P_{L,avg} = 1.5$  kW. Pulses with a duration of  $t_p = 30$  ns are emitted with a repetition rate between  $f = 5$  kHz and  $f = 50$  kHz at a wavelength of  $\lambda = 1030$  nm. An optical fibre diameter of  $d_f = 600$   $\mu\text{m}$  is required to enable the handling of the maximum pulse energy of  $E_p = 80$  mJ. A programmable focusing optic with integrated focus-shift (PFO-3D) is used as scanning optic. With objective lenses with a focal length of  $l_f = 255$  mm the resulting focal diameter is  $d_{focal} = 1.2$  mm and the available elliptical scan field has the dimensions of  $A_{sf} = 102$  mm x 174 mm. The resulting beam profile is a top-head profile with a homogenous energy distribution. During the investigations a cross-jet, run with pressured air, was used to protect the objective lenses. The process emissions were captured next to the processing zone.

In preparation of the laser processing a design of experiment (DoE) approach was taken to determine the parameters to be evaluated. A face-centered composite design with three variables scanning velocity  $v$ , hatch distance  $h$ , and number of repetitions  $\#$  was chosen. Each variable was appointed three values, cf. table 1.

Table 1. DoE parameters

DoE variables	symbol	Unit	Values		
scanning velocity	$v$	m/s	0.5	1	3
hatch distance	$h$	$\mu\text{m}$	200	600	1000
number of repetitions	$\#$	-	20	30	50

Other process parameters were kept constant during the experiment. Pulse energy was set to  $E_p = 80$  mJ at a frequency of  $f = 18.8$  kHz delivering  $P_L = 1.5$  kW. The process was paused after each repetition for a break of  $t_b = 0.5$  s.

An epoxy based crimped CFRP fabric with twill-weave and a thickness of  $d = 3$  mm was used for the investigations. Material samples were cut to approx.  $A_{init} = 50 \times 50$   $\text{mm}^2$ , three pieces per set of parameters. Then the samples' dimensions and weight were measured using a calliper and a precision balance.

For the investigations, an area with a size of  $A_{proc} = 40 \times 40$   $\text{mm}^2$  was ablated. After laser processing the remaining weight of the sample was measured again with a precision balance.

In a second investigation in order to evaluate the HAZ that was established during laser processing, micro-cross-sections were produced and analysed using optical microscopy.

### 3. Results

The samples were weighed and measured before processing. For each sample the individual results were recorded. On average, a sample weighed approx.  $m = 13.5 \text{ g}$ , had a volume of  $V = 9 \text{ cm}^3$ , and a density of  $\rho = 1.5 \text{ mg/mm}^3$ .

During laser processing of the samples, the laser control software logged the processing time  $t$ . In figure 1 the process time for the thirteen process parameter sets are shown.

After processing the removed material's volume  $V_r$  was determined by measuring the sample's remaining weight  $m$  and using its calculated density  $\rho$ . Parameter sets 3, 6, 7, and 10 produced enough total energy to remove the complete CFRP sheet's thickness  $d = 3 \text{ mm}$  before the scheduled end of process. Therefore, the removed material volume  $V_r$  could not be determined for these parameter sets. For the remaining samples  $V_r$  is shown in figure 2.

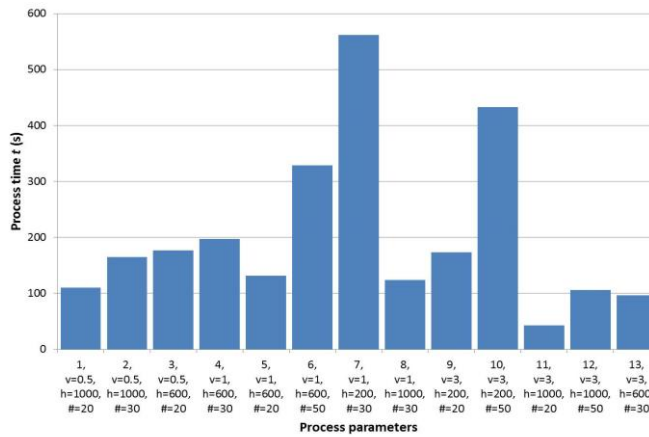


Fig. 1. Recorded process times for tested parameter sets.

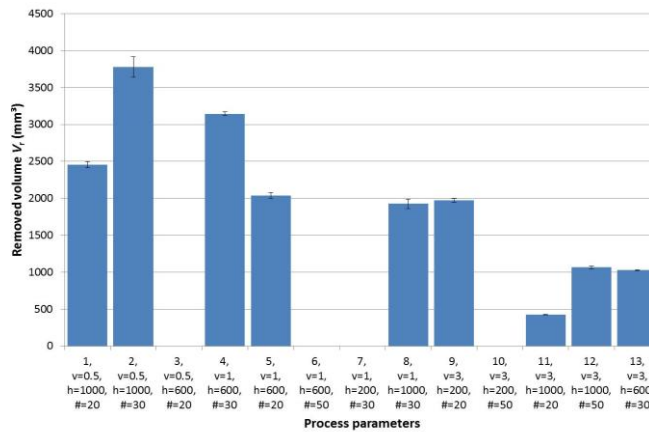


Fig. 2. Amount of removed CFRP. Parameter sets 3, 6, 7, and 10 completely removed all the material before the process ended.

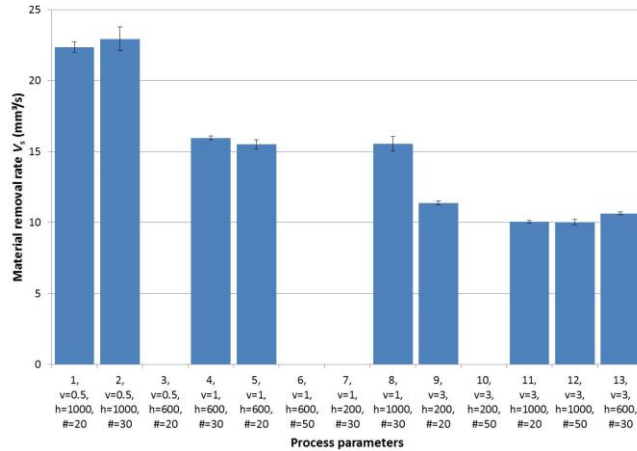


Fig. 3. Material removal rates for the tested parameter sets. Parameter sets 3, 6, 7, and 10 completely removed all the material before the process ended.

The bulk material removal rate  $V_s$  was calculated with regard to  $V_r$  and  $t$ . The results are shown in figure 3. Again, for parameters 3, 6, 7, and 10  $V_s$  was not determined due to the missing  $V_r$ .

According to figure 3 slow scanning velocities and large hatch distances lead to a high material removal rate. In order to better identify the influence of the single parameters  $v$ ,  $\#$ , and  $h$  on the process result,  $V_s$  was entered as the result into the DoE. Only those nine results were evaluated that had a determinable material removal. A cubic polynomial approach was used to calculate the effect plots.

The effect plot for  $V_s$  (cf. figure 4) shows that the volume rate decreases with increasing scanning velocity. For scanning velocities slower than  $v = 1$  m/s, the material removal rate  $V_s$  is above the average of the tested parameters ( $V_s > 15$  mm³/s). For hatch distances  $h > 700$   $\mu$ m the material removal rate is more effective than average and keeps rising almost linearly. This is unexpected, as a large hatch distance would be expected to result in smaller line overlap and less delivered energy. It is assumed that a minor material removal per repetition at large hatch distances is compensated by a shorter processing time per repetition in comparison to a high material removal per repetition at short hatch distances and a longer process time per repetition.

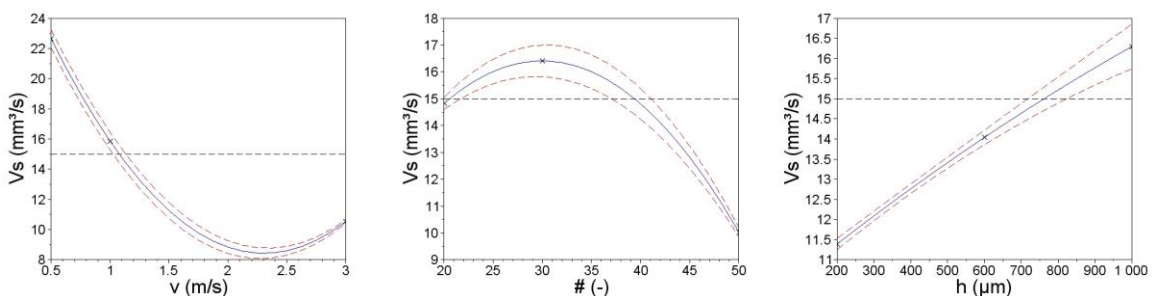


Fig. 4. Effect plots of scanning velocity, number of repetitions, and hatch distance for processing time.

The samples produced for cross-section analysis were cut into smaller pieces of approx.  $A_{\text{cross}} = 20 \times 25 \text{ mm}^2$  and embedded in resin. Using optical microscopy the HAZ was identified as a particularly white area on top of the ablated surface (z-direction) and the cutting edges (x/y-plane), cf. figure 5.

Comparable to the experience of cutting experiments the scanning velocity has a big influence in the appearance of the HAZ. The reduction of the scanning velocity has a direct influence on the HAZ at the bottom of the scarf as well as to the sides.

The analysis of the HAZ shows only small amounts of affected fibre and matrix material. The extent of the HAZ was determined by measuring its average width (x/y-plane) and height (z-direction). In general, the visible extent of the HAZ was bigger in x/y-plane than in z-direction. This is due to the carbon fibres' high heat conductivity coefficient in fibre direction.

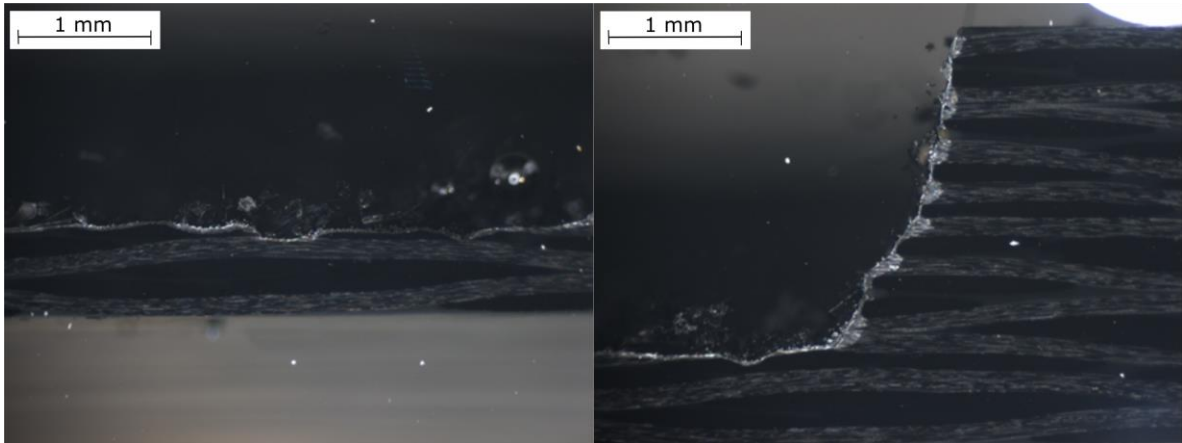


Fig. 5. Cross-section with HAZ on average of 0.023 mm (z-direction, left picture) and 0.025 mm (x/y-plane, right picture) for  $v = 1 \text{ m/s}$ .

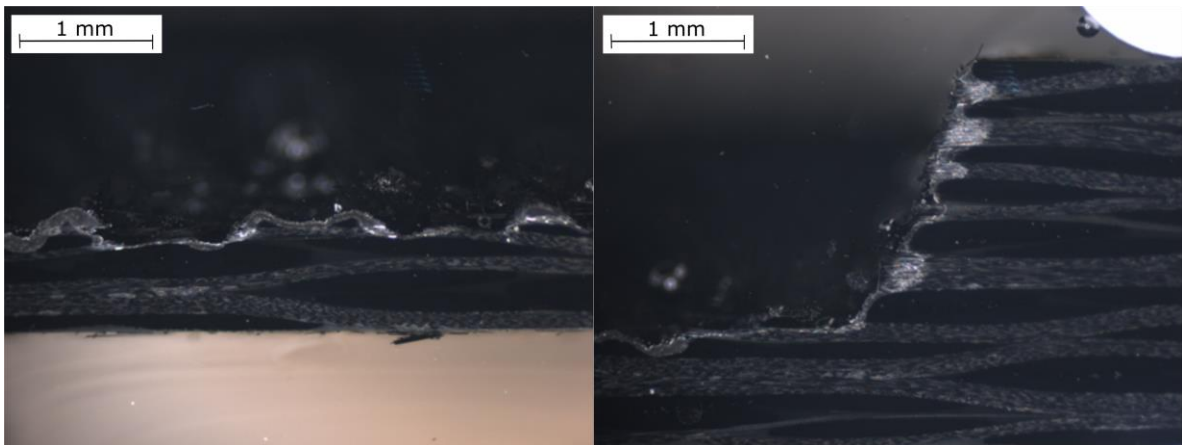


Fig. 6. Cross-section with HAZ on average of 0.095 mm (z-direction, left picture) and 0.076 mm (x/y-plane, right picture) for  $v = 0.1 \text{ m/s}$ .

#### 4. Conclusion

The HAZ that was detected during this investigation varied between 14  $\mu\text{m}$  and 129  $\mu\text{m}$ . For the HAZ in x/y-plane, it has been shown by Bluemel et al., 2015 for laser cutting of CFRP that a width of 200  $\mu\text{m}$  is tolerable for automobile applications. The height of the HAZ appears to be comparably small with approx. 20-30  $\mu\text{m}$ , but there has not been an analysis of its influence on the strength of a repaired CFRP part yet. This will be part of future analysis.

The investigations showed that this high-power laser achieved very high material removal rates (approx.  $V_s = 15 \text{ mm}^3/\text{s}$  on average) in comparison with lasers used in earlier research. Especially for laser based repair preparation this is a significant step forward. While this is still not on the same level as conventional milling in terms of pure processing time yet, the laser process benefits from not requiring any tool changes. Also, the efficiency and precision of this laser process can be further increased by optical measurements. Adding online optical coherence tomography for depth measurements will allow to precisely ablate CFRP plies and allow the precise insertion of repair patches into the laser prepared scarf area. For unidirectional CFRP, fibre orientation measurements can be performed during the laser process. This will enable a layer-by-layer removal of the damaged CFRP that will also be able to react to imperfections in the material like undulations that stem from the production process. Both technologies are able to significantly improve the laser based repair process and advance it towards full automation.

#### Acknowledgements

The data presented here results from work performed in the BMBF project "HolQueSt 3D – 3D Hochleistungs-Laserbearbeitung zur Qualitäts- und Durchsatzsteigerung für die prozesssichere, automatisierte Fertigung von CFK-Leichtbau-Strukturen" and LuFo V-2 project "ReWork – Prozesssicheres ReWork an dünnwandigen, gekrümmten CFK-Oberflächen mittels photonischer Systeme und piezo-gestützter Qualitätskontrolle". The authors would like to express their gratitude towards the German Federal Ministry for Economic Affairs and Energy (BMWi) for funding the research conducted in ReWork subproject "Optimierung der laserbasierten Oberflächennachbearbeitung von CFK-Bauteilen durch präzisen, lagenweisen Materialabtrag" (20Q1521B) as well as towards the German Federal Ministry of Education and Research (BMBF) for funding the research conducted in HolQueSt 3D subproject "Entwicklung eines Prozesses zur CFK-Bearbeitung auf Basis eines fasergeführten Hochleistungslasers mit Pulsdauern im Nanosekundenbereich" (13N12763).

#### References

- Bluemel, S., Bastick, S., Staehr, R., Jaeschke, P., Suttman, O., Overmeyer, L., 2016. Laser Cutting of CFRP with a Fibre Guided High Power Nanosecond Laser Source – Influence of the Optical Fibre Diameter on Quality and Efficiency, *Physics Procedia* 83, pp. 328–335.
- Bluemel, S., Angrick, V., Bastick, S., Jaeschke, P., Suttman, O., Overmeyer, L., 2015. Remote Laser Cutting Of Composites With A Fibre Guided Thin-Disk Nanosecond High Power Laser. *Proceedings of Lasers in Manufacturing. Lasers in Manufacturing Conference. München. 22-25 June.*
- Dittmar, H., Gäbler, F., Stute, U., 2013. UV-laser ablation of fibre reinforced composites with ns-pulses. *Physics Procedia* 41, pp. 266-275.

- Kremser, B., Ziolkowski, E., Friedel, S., Roehner, M., Stolberg, K., Freyhold, N. v., 2014. Processing of lightweight materials with high peak power ns-pulsed disk lasers. Proceedings LANE 2014. 8th International Conference on Photonic Technologies LANE 2014. Fürth.
- Stolzenburg, C., Schüle, W., Angrick, V., Bouzid, M., Killi, A., 2014. Multi-kW IR and green nanosecond thin-disk lasers. SPIE LASE Proceedings Volume 8959. San Francisco, California, United States. Saturday 1 February 2014, p. 89590.
- Wolynski, A., Herrmann, T., Mucha, P., Haloui, H., L'huillier, J., 2011. Laser ablation of CFRP using picosecond laser pulses at different wavelengths from UV to IR, Physics Procedia 12, p. 292–301.
- Zahedi, E., Freitag, C., Wiedenmann, M., Onuseit, V., Weber, R., Graf, T., 2015. HIGH ABLATION RATE LASER PROCESSING OF CFRP FOR REPAIR PURPOSE. Proceedings of ICALEO 2015. International Congress on applications of lasers & electro-optics. Atlanta. 18-22 October.